

# A distributed control algorithm for the minimization of the power generation cost in smart micro-grid

Guido Cavraro, Ruggero Carli, and Sandro Zampieri

**Abstract**— We consider the problem of minimizing the power generation cost by exploiting the distributed renewable energy sources (DRES) located in the power distribution network. The proposed strategy requires that the intelligent agents, located at the microgenerator buses, measure their voltage and then adjust the amount of injected power, according to a feedback control law that is indeed a projected gradient descent strategy. Simulations are provided in order to illustrate the algorithm behavior.

## I. INTRODUCTION

The ultimate goal of the optimal power flow (OPF) problem is to find an operating point of the power system that minimizes a cost function (typically the generation cost or the line losses) satisfying the power demand and some operative constraints, such as bus voltage limits or generators generation limits. In the past, algorithms for the solution of the OPF problem have been applied to the transmission networks, namely, the high voltage networks transporting the electrical power from the power plants to the distribution networks and finally to the users.

The advent of distributed energy resources such as wind turbines, solar cells, or other renewable energy sources is drastically changing the actual power distribution scenario [1]. In the near future, several agents (the *prosumers* [2]) on the power grid will be able to have generation capacity, storage capacity and loads. In fact, a massive number of small power generators are envisioned to be deployed in the low voltage and medium voltage power distribution grid. The availability of this large number of generators will yield to a number of benefits for the electrical distribution system, such as voltage profile improvements, reduction of line losses and power generation cost and other ancillary services [3]. On the other hand, power injection of several renewable energy sources could lead, if not properly regulated, to system instability, thus requiring the solution of OPF problems also in the low and medium voltage power distribution networks.

In the traditional transmission grid the OPF problem is typically solved by centralized solvers that collect all the necessary field data, compute the optimal configuration, and dispatch the power production to the generators. However this approach is not practical in the distribution network, due to the fast variability in the power demand, to the poor prediction on small size generators energy production and to the fact that generators can connect or disconnect, requiring

an automatic reconfiguration of the grid control infrastructure (the so called “plug and play” approach).

Many algorithms solving the OPF problem have been designed. Many of them exploit a powerful optimization technique, the ADMM ([4]). They typically require a large number of iterations and a high computational burden to converge, mainly due to the nonlinear relations among powers and voltages which make the OPF problem non-convex. To overcome these drawbacks, one of the most popular solution is to reformulate the OPF problem as a rank-constrained semidefinite program, which is convexified by dropping the rank constraint and it is finally solved in a distributed manner, via a primal or dual optimization ([5]) or via the ADMM ([6]). However all these approaches are based on the standing assumptions that all the buses of the grid are monitored and all the grid parameters (topology, line impedances etc.) are perfectly known; these assumptions might be unrealistic in many scenarios. Additionally, the OPF solution is applied only after a number of communication rounds which are needed by the optimization process to provide the solution.

The algorithm we propose, extends the approach of [7] and [8] to the OPF problem, and can be considered as a feedback control strategy. Indeed, its key feature is the alternation between measurement steps and actuation steps which are based on the measured data (phasorial voltages), and therefore it is inherently an online algorithm. This fact is particularly important as it allows to chase the power demand and the generation capability variation, that in presence of renewable energy sources are highly changing. Remarkably, the algorithm we propose is guaranteed to converge to a quasi optimal solution without monitoring all the grid nodes, but only the generators.

In the OPF problem we consider, the goal is to minimize the global generation cost by controlling the amount of active powers injected in the grid by the generators. The active powers are subject to box constraints modeling the generation capability of each generator, while the objective function is given by the sum of the generation cost functions associated to the generators. In our setup we consider only two types of such functions: the ones associated to the micro-generators dispersed in the grid and the one associated to the utility. We tackle the problem via a projected gradient-based approach. In particular exploiting an approximated solution of the power flow nonlinear equations, we show the gradient of the objective function can be computed by the composites just via local measurements of the phasorial voltages at their connection points. Applying at each iteration a projected gradient descent step, the algorithm is shown to be provably convergent to an approximated optimal solution

The authors are with the Dept. of Information Engineering, University of Padova, Via Gradenigo 6/a, 35131 Padova, Italy. Email: {cavraro, carli, rug, zampieri}@dei.unipd.it. The research leading to these results has received funding from the European Community's Seventh Framework Program under grant agreement n. 257462 HYCON2 Network of Excellence.

of the OPF problem. Furthermore, we provide a characterization of the optimal solution that can be useful to design algorithms that solve the OPF problem.

## II. MATHEMATICAL PRELIMINARIES AND NOTATION

Let  $\mathcal{G} = (\mathcal{V}, \mathcal{E}, \sigma, \tau)$  be a directed graph, where  $\mathcal{V}$  is the set of nodes,  $\mathcal{E}$  is the set of edges, with  $n = |\mathcal{V}|, r = |\mathcal{E}|$ . Moreover  $\sigma, \tau : \mathcal{E} \rightarrow \mathcal{V}$  are two functions such that edge  $e \in \mathcal{E}$  goes from the source node  $\sigma(e)$  to the terminal node  $\tau(e)$ . In the paper we introduce complex-valued functions defined on the nodes and on the edges. These functions will also be intended as vectors in  $\mathbb{C}^n$  and  $\mathbb{C}^r$ . Given a vector  $u$ , we denote by  $\bar{u}$  its (element-wise) complex conjugate, and by  $u^T$  its transpose. We denote by  $\Re(u)$  and by  $\Im(u)$  the real and the imaginary part of  $u$ , respectively. Let  $A \in \{0, \pm 1\}^{r \times n}$  be the incidence matrix of the graph  $\mathcal{G}$ , defined via its elements

$$[A]_{ev} = \begin{cases} -1 & \text{if } v = \sigma(e) \\ 1 & \text{if } v = \tau(e) \\ 0 & \text{otherwise.} \end{cases}$$

We define as  $\mathbf{1}$  the column vector of all ones, while  $\mathbf{1}_v$  is the vector whose value is 1 in position  $v$ , and 0 everywhere else. Given  $u, v, w \in \mathbb{R}^\ell$ , with  $v_h \leq w_h, h = 1, \dots, \ell$  we define the operator  $\text{proj}(u, v, w)$  as the component wise projection of  $u$  in the set  $\{x \in \mathbb{R}^\ell : v_h \leq x_h \leq w_h, h = 1, \dots, \ell\}$ , i.e.,

$$[\text{proj}(u, v, w)]_h = \begin{cases} u_h & \text{if } v_h \leq u_h \leq w_h \\ v_h & \text{if } u_h < v_h \\ w_h & \text{if } u_h > w_h \end{cases} \quad (1)$$

## III. CYBER-PHYSICAL MODEL OF A SMART GRID

In this paper, we envision a *smart* power distribution network as a cyber-physical system, in which the *physical layer* is the power distribution infrastructure, including power lines, microgenerators, loads and the point of connection to the transmission grid (PCC), and the *cyber layer* consists of intelligent agents, scattered in the electrical network, and provided with actuation, communication, sensing, and computational capabilities. We use a directed graph  $\mathcal{G} = (\mathcal{V}, \mathcal{E})$  to model the physical layer, where nodes in  $\mathcal{V}$  represent both loads and generators that are connected to the microgrid and edges in  $\mathcal{E}$  represent the power lines. We limit our study to the steady state behavior of the system, where all voltages and currents are sinusoidal signals waving at the same pulsation  $\omega_0$ , and can therefore be represented in phasorial notation.

The system state is described by the following system variables:

- $u \in \mathbb{C}^n$ , where  $u_v$  is the grid voltage at node  $v$ ;
- $i \in \mathbb{C}^n$ , where  $i_v$  is the current injected at node  $v$ ;
- $s = p + iq \in \mathbb{C}^r$ , where  $s_v, p_v$  and  $q_v$  are the complex, the active and the reactive power injected at node  $v$ .

We assume that every microgenerator, and also the PCC, corresponds to an *prosumer* in the cyber layer. We denote this subset of the nodes of  $\mathcal{G}$  by  $\mathcal{C}$  (with  $|\mathcal{C}| = m$ ). Each prosumer (referred to also as agent) is provided with sensing capability in the form of a phasor measurement unit (PMU, i.e., a sensor measuring voltage amplitude and angle [9]). Agents that correspond to microgenerators can command

the amount of power injected in the grid. Moreover agents can communicate with each other, via some communication channels which could possibly via power line communication (PLC). We introduce the following block decomposition for the vectors of voltages  $u$  and powers  $s$

$$u = [u_0 \quad u_G \quad u_L]^T, \quad s = [s_0 \quad s_G \quad s_L]^T, \quad (2)$$

where  $u_0$  is the voltage at the PCC,  $u_G \in \mathbb{C}^{m-1}$  and  $u_L \in \mathbb{C}^{n-m}$  are the voltages at the microgenerators and at the loads, respectively. Similarly for  $s_G = p_G + jq_G$  and  $s_L = p_L + jq_L$ . We denote, for every edge  $e$  of the graph, by  $z_e$  the impedance of the corresponding power line. We assume the following.

*Assumption 1:* All power lines in the grid have the same inductance/resistance ratio, i.e.,  $z_e = e^{j\theta}|z_e|$ , for any  $e$  in  $\mathcal{E}$  and for a fixed  $\theta$ .

Assumption 1 is satisfied when the grid is relatively homogeneous, and is reasonable in most practical cases. We collect all the grid impedances absolute values in the matrix  $Z = \text{diag}(|z_e|, e \in \mathcal{E})$ . We label the PCC as node 0 and take it as an ideal sinusoidal voltage generator (*slack bus*) at the microgrid nominal voltage  $U_N$ , with arbitrary, but fixed, angle  $\phi$ . We model all nodes but the PCC as *constant power* or *P-Q buses*. The powers  $s_v$  corresponding to grid loads are such that  $p_v < 0$ , meaning that positive active power is *supplied* to the devices. On the other hand, the complex powers corresponding to microgenerators are such that  $p_v \geq 0$ , as positive active power is *injected* into the grid. It is known that the system state satisfies the equations

$$u = e^{-i\theta} Y i \quad (3)$$

$$u_0 = U_N e^{i\phi} \quad (4)$$

$$u_v i_v = p_v + iq_v \quad v \neq 0 \quad (5)$$

where  $Y := A^T Z^{-1} A$  is the matrix collecting the absolute values of the bus admittance matrix of the grid. From now on, we consider, without loss of generality,  $\phi = 0$ . The following Lemma (that can be found in [10]) will be useful in the sequel.

*Lemma 2:* Given  $Y := A^T Z^{-1} A$ , there exists a unique symmetric, positive semidefinite matrix  $X \in \mathbb{R}^{n \times n}$  such that

$$\begin{cases} XY = I - \mathbf{1}\mathbf{1}_0^T \\ X\mathbf{1}_0 = 0. \end{cases} \quad (6)$$

The matrix  $X$  depends only on the topology of the grid power lines and on their impedances and, adopting the same block decomposition as in (2), we can write

$$X = \begin{bmatrix} 0 & 0 & 0 \\ 0 & M & N \\ 0 & N^T & Q \end{bmatrix}, \quad (7)$$

with  $M \in \mathbb{R}^{(m) \times (m)}$ ,  $N \in \mathbb{R}^{(m) \times (n-m-1)}$ , and  $Q \in \mathbb{R}^{(n-m-1) \times (n-m-1)}$ . We have therefore

$$u = e^{i\theta} X i + \mathbf{1} U_N. \quad (8)$$

We conclude this section by introducing a useful approximated solution of the nonlinear equations (3), (4), and (5), that, again, can be found in [10].

*Proposition 3:* Consider the physical model described by the set of nonlinear equations (3), (4), (5) and (8). Node voltages then satisfy

$$\begin{bmatrix} u_0 \\ u_G \\ u_L \end{bmatrix} = U_N \mathbf{1} + \frac{e^{j\theta}}{U_N} \begin{bmatrix} 0 & 0 & 0 \\ 0 & M & N \\ 0 & N^T & Q \end{bmatrix} \begin{bmatrix} 0 \\ \bar{s}_G \\ \bar{s}_L \end{bmatrix} + o\left(\frac{1}{U_N}\right) \quad (9)$$

(the little-o notation means that  $\lim_{U_N \rightarrow \infty} \frac{o(f(U_N))}{f(U_N)} = 0$ ).

#### IV. OPTIMAL POWER FLOW PROBLEM

The goal of this paper is to design a distributed control algorithm that leads to the minimization of the power generation cost of the power supplied to the loads, that we assume to be constant power loads requiring  $\hat{s}_L$ . Formally the problem we are interested into can be stated as

$$\min_{s_j, j \in \mathcal{C} \cup \text{PCC}} f = \sum_{j=1}^m f_j(p_j) + f_0(p_0) \quad (10a)$$

$$\text{s.t. } s_L = \hat{s}_L \quad (10b)$$

$$p_0 = -(\mathbf{1}^T p_G + \mathbf{1}^T p_L) + \ell(s_G, s_L, U_N) \quad (10c)$$

$$0 \leq p_v \leq p_v^M \quad v \in \mathcal{C} \quad (10d)$$

where

- constraint in (10c) models the active power conservation in the grid, being  $\ell(s_G, s_L, U_N)$  the active power losses in the grid;
- constraints in (10d) model the agents generation capabilities;
- the objective function  $f$  is the sum of the cost of the power produced by the utility and injected into the microgrid through the PCC ( $f_0(p_0)$ ), and of the microgenerators' payments for the power that they inject.

Observe that (10c) provides a expression of  $p_0$  as a function of  $s_G, s_L, U_N$  (in the following  $p_0$  or  $p_0(p_G)$  stand for  $p_0(s_G, s_L, U_N)$ ). We define  $\mathcal{B}$  as the feasible set, that is

$$\mathcal{B} = \{p_G \in \mathbb{R}^m : 0 \leq p_v \leq p_v^M\}.$$

In several studies of the OPF problem and in recent papers [11], [12], [13], the cost functions are typically chosen quadratic (e.g  $f_j(p_j) = \alpha_j^2 p_j^2 + \alpha_j^1 p_j + \alpha_j^0$ ), or anyway convex, continuous and differentiable, because they derive from models of the energy production costs of classical power plants and generators. However these choices do not capture the features of scenarios with high penetration of distributed renewable energy resources (DRES), such as photovoltaic panels, that produce energy at zero cost, but whose owners receive a reward from the utility for the energy they inject into the grid. In this new scenario the cost function does not model anymore the effective cost of energy production, but rather the retribution that the prosumers receive. Typically the reward is proportional to the quantity of energy injected into the grid, with a proportionality constant that depends on the contractual agreement among the producer and the utility. This reward can be modeled as

$$f_j(p_j) = \begin{cases} c_G^j p_j & p_j \geq 0 \\ 0 & p_j < 0 \end{cases} \quad \forall j \in \mathcal{C} \quad (11)$$

since, obviously if the power produced  $p_j^p$  by the prosumer  $j$  is lower than the power that it requires  $p_j^r$ , it has to pay the difference  $p_j = p_j^p - p_j^r < 0$  and then it is not rewarded.

In this framework there are mainly two possible scenarios. The first one is related to the ‘‘prosumers point of view’’. Since the prosumers are paid proportionally to the energy that they inject and since their production basically has no cost, they would like to maximize the power they inject, while keeping satisfied some operative constraints. The result is a game among the agents. A first treatment on this scenario can be found in [14].

The second scenario is instead related to the ‘‘utility point of view’’, where the total cost accounts for the production cost of the energy injected by the PCC (that comes from big generation plants such as nuclear or hydroelectrical plants) and for the remuneration to be paid to the owners of DRES. In this framework, the utility imposes a behaviour procedure to be followed by the prosumers to compute the amount of energy they have to inject into the grid: the goal of the utility is to minimize the total cost while satisfying some operative constraints.

In this paper we focus on the second scenario. As it will be clear in the following, the utility, differently from the classical centralized schemes, does not impose to the agents the active power reference points (and even does not know them). But it just provides them the informations needed to compute and to actuate (all by their own) the optimal power input.

We assume for simplicity that all the agents are paid in the same way, that is,

$$c_G^j = c_G \quad \forall j \in \mathcal{C}$$

and we model  $f_0(p_0)$  as the  $f_j, j \in \mathcal{C}$ , that is

$$f_0(p_0) = \begin{cases} c_0 p_0 & p_0 \geq 0 \\ 0 & p_0 < 0 \end{cases} \quad (12)$$

However our treatment can be easily generalized to the case in which the reward is different from one producer to another and in which either the reward or the power generation cost at the PCC are modeled with different functions.

Based on (9) and by exploiting the properties of  $X$  we can express the active power losses in the grid as

$$\begin{aligned} \ell(s_G, s_L, U_N) &= \left( [p_G^T \quad p_L^T] \begin{bmatrix} M & N \\ N^T & Q \end{bmatrix} \begin{bmatrix} p_G \\ p_L \end{bmatrix} + \right. \\ &\quad \left. + [q_G^T \quad q_L^T] \begin{bmatrix} M & N \\ N^T & Q \end{bmatrix} \begin{bmatrix} q_G \\ q_L \end{bmatrix} \right) \frac{\cos(\theta)}{U_N^2} + o\left(\frac{1}{U_N^2}\right) \end{aligned} \quad (13)$$

Defining

$$\begin{aligned} \tilde{\ell}(s_G, s_L, U_N) &= \left( [p_G^T \quad p_L^T] \begin{bmatrix} M & N \\ N^T & Q \end{bmatrix} \begin{bmatrix} p_G \\ p_L \end{bmatrix} + \right. \\ &\quad \left. + [q_G^T \quad q_L^T] \begin{bmatrix} M & N \\ N^T & Q \end{bmatrix} \begin{bmatrix} q_G \\ q_L \end{bmatrix} \right) \frac{\cos(\theta)}{U_N^2} \end{aligned} \quad (14)$$

we can rewrite (10c) as

$$\begin{aligned} p_0 + \mathbf{1}^T(p_G + p_L) &= \ell(s_G, s_L, U_N) \\ &\simeq \tilde{\ell}(s_G, s_L, U_N). \end{aligned}$$

Hence we can approximate problem (10) with the following one

$$\min_{s_j, j \in \mathcal{C}} \hat{f} \quad (15a)$$

$$\text{s.t. } s_L = \hat{s}_L \quad (15b)$$

$$\hat{p}_0 = -(\mathbf{1}^T p_G + \mathbf{1}^T p_L) + \tilde{\ell}(s_G, s_L, U_N) \quad (15c)$$

$$0 \leq p_v \leq p_v^M \quad v \in \mathcal{C} \quad (15d)$$

where

$$\hat{f} = c_G \mathbf{1}^T p_G + f_0(-\mathbf{1}^T p_G - \mathbf{1}^T p_L + \tilde{\ell}(s_G, s_L, U_N))$$

and where  $\hat{p}_0$  is an approximation of  $p_0$  that differs from it just up to infinitesimal terms. Observe that problem (15) is convex. It is convenient to express  $\hat{f}$  in the following way:

$$\hat{f}(p_G) = \begin{cases} \hat{f}^+(p_G) & \text{if } p_G \in \mathcal{P}^+ \\ \hat{f}^-(p_G) & \text{if } p_G \in \mathcal{P}^- \end{cases} \quad (16)$$

where

$$\begin{aligned} \hat{f}^+(p_G) &= (c_G - c_0) \mathbf{1}^T p_G + c_0 \tilde{\ell}(s_G, s_L, U_N) \\ \hat{f}^-(p_G) &= c_G \mathbf{1}^T p_G \\ \mathcal{P}^+ &= \{p_G : -\mathbf{1}^T p_G - \mathbf{1}^T p_L + \tilde{\ell}(s_G, s_L, U_N) > 0\} \\ \mathcal{P}^- &= \{p_G : -\mathbf{1}^T p_G - \mathbf{1}^T p_L + \tilde{\ell}(s_G, s_L, U_N) \leq 0\} \end{aligned}$$

i.e.,  $\mathcal{P}^+$  is the set of all the  $p_G$  such that  $\hat{p}_0(p_G) > 0$ , while  $\mathcal{P}^-$  is the set of all the  $p_G$  such that  $\hat{p}_0(p_G) < 0$ . We furthermore define

$$\mathcal{P}^0 = \{p_G : -\mathbf{1}^T p_G - \mathbf{1}^T p_L + \tilde{\ell}(s_G, s_L, U_N) = 0\}$$

i.e., the set of all the  $p_G$  such that  $\hat{p}_0(p_G) = 0$ .

We conclude this section with a characterization of the optimal solution of (10).

*Proposition 4:* Consider problem (10). If  $p_G^*$  is an optimal solution, then  $p_0(p_G^*) \geq 0$ .

*Proof:* Let  $p_G^*$  be an optimal solution such that  $p_0^* = p_0(p_G^*) \leq 0$  and let  $\ell_A(s_G^*, s_L^*, U_N)$  be the active power losses of the system in this configuration. We will show that there exist another configuration  $\tilde{p}_G$  such that  $f(\tilde{p}_G) < f(p_G^*)$  and  $\tilde{p}_0 = p_0(\tilde{p}_G) \geq p_0^*$ . If  $p_0^* < 0$ , from (10c), it follows that there exist at least a compensator  $k$  such that  $p_k > 0$ . Let now  $k$  decrease its active power injection by  $-\delta_k$ ,  $\delta_k > 0$ . Let  $\delta_k$  such that

$$p_0(p_G^*) \leq p_0(p_G^* - \mathbf{1}_k \delta_k) \leq 0.$$

Now let us examine the change  $\Delta i_0$  in the current injected by the PCC. We have

$$\begin{aligned} \Delta i_0 &= \mathbf{1}_0^T Y \Delta u \\ &= \mathbf{1}_0^T Y X (\mathbf{1}_0 - \mathbf{1}_k) \frac{\delta_k}{U_N^2} + o\left(\frac{1}{U_N}\right) \\ &= \mathbf{1}_0^T (I - \mathbf{1}_0 \mathbf{1}^T) (\mathbf{1}_0 - \mathbf{1}_k) \frac{\delta_k}{U_N^2} + o\left(\frac{1}{U_N}\right) \\ &= \frac{\delta_k}{U_N^2} + o\left(\frac{1}{U_N}\right) \simeq \frac{\delta_k}{U_N^2} \end{aligned}$$

It follows that the active power absorption of the PCC after the injection drop  $\delta_p$  changes by

$$\Delta p_0 = \Re(U_N \Delta \xi_e) = U_N \frac{\delta_k}{U_N} > 0$$

that is,  $p_0(p_G^* - \mathbf{1}_k \delta_k, q_G^*) > p_0(p_G^*)$ . Finally, we point out that the new configuration, with a greater  $p_0$  has a cost that is lower than the starting one:

$$\begin{aligned} \hat{f}(p_G - \mathbf{1}_k \delta_k) - \hat{f}(p_G) &= \\ &= -c_G \delta_k + f_0(p_G - \mathbf{1}_k \delta_k, q_G) - f_0(p_G, q_G) \\ &\simeq -c_G \delta_k \leq 0 \end{aligned}$$

The same proof can be applied also if we consider problem (15) instead of (10). The above proposition implies that the optimal solution  $p_G$  belongs to  $\mathcal{P}^+ \cup \mathcal{P}^0$ . Moreover, using a reasoning similar to the one exploited in the above proof, we can easily prove the following

*Lemma 5:* Consider problems (10) and (15), if  $p_0^* = 0$ , then  $c_0 > c_G$ .

#### V. A GRADIENT PROJECTED DESCENT ALGORITHM

The algorithm we propose is based on a gradient descent strategy that we derive considering the approximated problem (15). Let us compute the gradient of the cost function  $\hat{f}$ . Observe that

$$\frac{\partial \left( \sum_j^m f_j(p_j) \right)}{\partial p_G} = c_G \mathbf{1},$$

while, concerning  $\frac{\partial f_0(p_0)}{\partial p_j}$ , by exploiting the chain rule we have that

$$\frac{\partial f_0(p_0)}{\partial p_G} = f_0'(p_0) \left( -\mathbf{1} + 2 \frac{\cos(\theta)}{U_N^2} (M p_G + N p_L) \right)$$

Plugging together the above expressions we get

$$\frac{\partial \hat{f}}{\partial p_G} = f_G'(p_G) + f_0'(p_0) \left( -\mathbf{1} + 2 \frac{\cos(\theta)}{U_N^2} (M p_G + N p_L) \right) \quad (17)$$

which, using (11) and (12), can be finally rewritten as

$$\frac{\partial \hat{f}}{\partial p_G}(p_G) = c_G \mathbf{1}, \quad (18)$$

if  $p_G \in \mathcal{P}^-$ , otherwise

$$\frac{\partial \hat{f}}{\partial p_G}(p_G) = 2c_0 \frac{\cos(\theta)}{U_N^2} (M p_G + N p_L) + (c_G - c_0) \mathbf{1} \quad (19)$$

if  $p_G \in \mathcal{P}^+$ .

Observe that, while the values  $U_N$  and  $\theta$  can be assumed known a priori, the quantities  $Mp_G + Np_L$  depend on all the active powers injected into the grid (also on the unmonitored active powers of the loads) and on the topology of the grid. However, by exploiting again (9), we have that

$$u_G = \frac{e^{i\theta}}{U_N} [M \quad N] \begin{bmatrix} p_G - iq_G \\ p_L - iq_L \end{bmatrix} + \mathbf{1}U_N + o\left(\frac{1}{U_N}\right)$$

from which it follows that

$$\Re(e^{-i\theta}(u_G - \mathbf{1}U_N)) = \frac{Mp_G + Np_L}{U_N} + o\left(\frac{1}{U_N}\right) \quad (20)$$

and then

$$\begin{aligned} \frac{\partial \hat{f}}{\partial p_G}(p_G) &\simeq f'_G(p_G) + f'_0(p_0) \left( -\mathbf{1} + \right. \\ &\quad \left. + 2\frac{\cos(\theta)}{U_N} \Re(e^{-i\theta}(u_G - \mathbf{1}U_N)) \right) \end{aligned} \quad (21)$$

where in this last expression we are neglecting the terms that vanish to 0 for large  $U_N$ . It turns out that the gradient of  $\hat{f}$  can be computed only by local voltage measurements. Indeed  $\forall k \in \mathcal{C}$  we have that

$$\begin{aligned} [\Re(e^{-i\theta}(u_G - \mathbf{1}U_N))]_k &= |u_k| \cos(\angle u_k - \theta) + \\ &\quad - |u_N| \cos(\angle u_N - \theta) \end{aligned}$$

and then each compensator, in order to obtain its component of  $\frac{\partial \hat{f}}{\partial p_G}$ , needs only to know its own voltage, the PCC voltage and  $f'_0(p_0)$ . Next we formally describe the algorithm we propose in this paper. For simplicity, in the following,  $[\hat{g}_p]_h$  denotes the component of the approximated gradient related to agent  $h$ .

Let  $\gamma$  be a positive scalar parameter. At every iteration of the algorithm, each agent  $h \in \mathcal{C} \setminus \{0\}$  executes the following operations in order:

- 1) senses the system obtaining its voltage phasorial measurement  $u_h$ ;
- 2) receives the PCC voltage phasorial measurement  $u_0 = U_N$ , the PCC active power injected  $p_0$  and the cost coefficient  $c_0$ ;
- 3) computes the approximated gradient direction

$$\begin{aligned} [\hat{g}_p]_h &= f'_h(p_h) + f'_0(p_0)(-\mathbf{1} + \\ &\quad + 2\frac{\cos \theta}{U_N} (|u_k| \cos(\angle u_k - \theta) - |u_N| \cos(\angle u_N - \theta))) \end{aligned} \quad (22)$$

- 4) computes the active power to be injected in the grid performing the following gradient descent steps

$$p_h \leftarrow p_h - \gamma[\hat{g}_p]_h \quad (23)$$

- 5) projects  $p_h$  into the feasible region and actuates the projected values

$$p_h \leftarrow \text{proj}(p_h, 0, p_h^M) \quad (24)$$

Based on the above description, it is clear what is the feedback scheme that underlies the procedure we propose: during each iteration each agent senses the grid, communicates with the PCC, computes the power set-point and then actuates it.

## VI. CONVERGENCE ANALYSIS

In this section we consider the gradient projected descent of  $\hat{f}$

$$p_G(t+1) = \text{proj}\left(p_G(t) - \gamma \frac{\partial \hat{f}}{\partial p_G}, 0, p_G^M\right) \quad (25)$$

in spite of its approximated version given in (22), (23) and (24), that we perform in practice.

We consider three different scenarios:

- 1) the one in which  $p_G^* \in \mathcal{P}^+$  and  $\frac{\partial \hat{f}^+}{\partial p_G}(p_G^*) = 0$ , that is the solution of (15) is equal to the global minimizer of  $\hat{f}^+$ ;
- 2) the one in which  $p_G^* \in \mathcal{P}^+$  and  $\frac{\partial \hat{f}^+}{\partial p_G}(p_G^*) \neq 0$ , that is the minimum point of  $\hat{f}^+$  is not the same of  $\hat{f}$  (in this case the minimum of  $\hat{f}^+$  lies outside the boundary of  $\mathcal{B}$ );
- 3) the one in which  $p_G^* \in \mathcal{P}^0$ , that is the minimum argument of  $\hat{f}$  is such that  $p_0(p_G^*) = 0$ ;

We were able to provide a formal proof of convergence of (25) only for the first scenario. However extensive numerical simulations suggest that (25) converges to the optimum also in the second scenario. Concerning the third scenario, we can prove the convergence of the continuous-time version of (25) (which corresponds to have a  $\gamma$  which tends to zero) by resorting to the tools of sliding mode control. The crucial point is to theoretically quantify the difference among the continuous-time trajectory and the discrete-time trajectory. These considerations are summarized in the following propositions.

*Proposition 6:* Consider the optimization problem (15) and the dynamic system described by the update equation (25). Let  $p_G^*$  be the optimal configuration and assume that  $p_G^* \in \mathcal{P}^+$  and  $\frac{\partial \hat{f}^+}{\partial p_G}(p_G^*) = 0$ . Then the trajectory  $t \rightarrow p_G(t)$  converges to the optimal value  $p_G^*$  if

$$\gamma \leq \frac{U_N^2}{\cos \theta \rho(M) c_0}.$$

*Proposition 7:* Consider the optimization problem (15) and the continuous-time version of the dynamic system described by the update equation (25). Let  $p_G^*$  be the optimal configuration and suppose that  $p_G^* \in \mathcal{P}^0$ . Then the continuous-time trajectory  $t \rightarrow p_G(t)$  converges to the optimal value  $p_G^*$ .

## VII. SIMULATIONS

The algorithm has been tested on the testbed IEEE 37 [15], which is an actual portion of 4.8kV power distribution network located in California. The load buses are a blend of constant-power, constant-current, and constant-impedance loads, with a total power demand of almost 2 MW of active power and 1 MVAR of reactive power (see [15] for the testbed data). The length of the power lines range from a minimum of 25 meters to a maximum of almost 600 meters. The impedance of the power lines differs from edge to edge, however, the inductance/resistance ratio exhibits a smaller variation, ranging from  $\angle z_e = 0.47$  to  $\angle z_e = 0.59$ . This

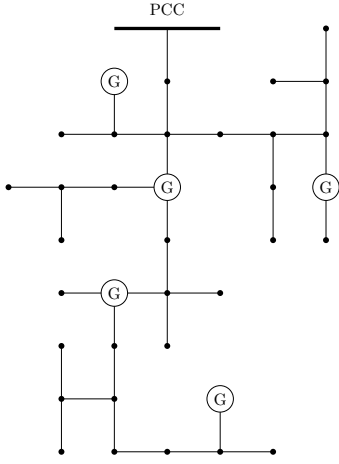


Fig. 1. Schematic representation of the IEEE 37 test feeder [15], where five microgenerators have been deployed.

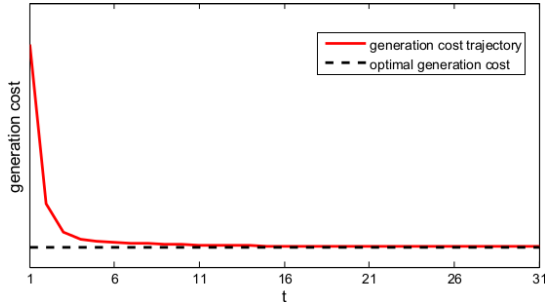


Fig. 2. Trajectory of a algorithm run, in which  $c_G/c_0 = 0.96$ .

justifies Assumption 1. We considered the scenario in which 5 microgenerators have been deployed in this portion of the power distribution grid (see Figure 1).

The maximum active power capabilities of each generator has been set to values that go from 85 to 490 kW. The algorithm presented in Section V have been simulated on a nonlinear exact solver of the grid [16].

Firstly, we simulate the first scenario, and we choose  $\gamma$  as one half of the bound indicated in the statement of Proposition 6. The results of the simulation have been plotted in Figure 2, in which we can see a smooth convergence. The parameter  $\gamma$  has been chosen as one half of the bound indicated by Proposition 6. The dashed blackline represents the cost of the OPF solution (computed via a numerical centralized solver that have access to all the grid parameters and load data) while the red line represents the behavior of the proposed algorithm. Finally, we simulate the case

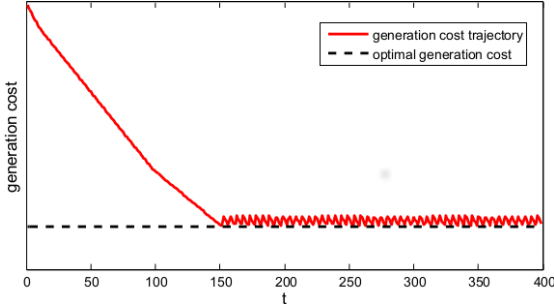


Fig. 3. Trajectory of a algorithm run, in the third scenario considered

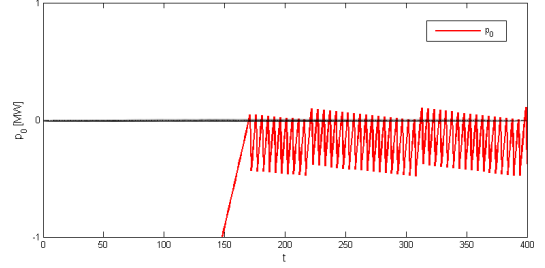


Fig. 4. Trajectory of  $p_0$  in the run depicted in Figure 3.

in which we are in the scenario treated by Proposition 7, and we choose  $\gamma$  as one hundredth of the bound indicated, in order to reduce the difference among the discrete-time and the continuous-time algorithm implementation. The cost trajectories is depicted in Figure 3, where it is clear the *chattering* typically produced by the sliding mode control near the optimal solution. In Figure 3 and most of all in Figure 4, where we plot the PCC active power injected trajectory, one can see that the “reaching phase” lasts around 150 iterations. In this phase, the  $p_G$ 's move towards  $\mathcal{P}^0$  until they cross it. Then it begins the sliding mode on  $\mathcal{P}^0$  with the characteristic chattering, and because of it  $p_0$  starts to chatter near zero.

## VIII. CONCLUSIONS AND FUTURE DEVELOPMENTS

In this paper we propose a feedback control strategy to solve the OPF problem in smart micro-grids with high penetration of DRES. We model the cost function, we state the OPF problem and we derive its convex approximation. Furthermore we characterize its optimal solution. Then we tackle the OPF problem by deriving a projected gradient ascent, and finally we provide some simulations in order to show and explain its behaviour. We envision as future plans to introduce in this framework also the control of reactive power, to deal with other operative constraints (such as node voltage magnitude) and to study the interaction among various micro-grid connected, by their PCC, to a higher level network (e.g. high voltage grid).

## APPENDIX

*Proof:* [Proof of Proposition 6]

In this scenario,  $p_G \in \mathcal{P}^+ \cap \mathcal{B}$ . Being  $p_G^*$  the solution of (15) and then a fixed point for (25), it satisfies

$$p_G^* = \left[ \left( I - \frac{2\gamma \cos(\theta) c_0}{U_N^2} M \right) p_G^* + \frac{2\gamma \cos(\theta)}{U_N^2} N p_L - \gamma (c_G - c_0) \mathbf{1} \right]_{\mathcal{P}^+} \quad (26)$$

where  $[\cdot]_{\mathcal{P}^+}$  is the projection into  $\mathcal{P}^+ \cap \mathcal{B}$ . Notice that the gradient of  $\hat{f}^+$  is a Lipschitz continous function, with Lipschitz constant  $K = \frac{2c_0 \cos \theta}{U_N^2} \rho(M)$ . In fact

$$\left\| \frac{\partial \hat{f}^+}{\partial p_G}(u) - \frac{\partial \hat{f}^+}{\partial p_G}(v) \right\| = \left\| \frac{2c_0 \cos \theta}{U_N^2} M(u - v) \right\| \leq \frac{2c_0 \cos \theta}{U_N^2} \rho(M) \|u - v\|$$

where  $\rho(M)$  is the spectral radius of  $M$ . Now, let's define  $d(t) = p_G(t) - p_G^*$ , and see what happens if we perform a projected gradient descent of  $\hat{f}$  with

$$\gamma \leq \frac{U_N^2}{2c_0 \cos \theta \rho(M)} \quad (27)$$

If  $p_G(t) \in \mathcal{P}^+$  then

- 1) the distance among  $p_G$  and  $p_G^*$  always decreases, that is

$$\|d(t+1)\| \leq \|d(t)\| \quad (28)$$

In fact

$$\begin{aligned} \|d(t+1)\| &= \|p_G(t+1) - p_G^*\| \\ &= \|p_G(t+1) - [p_G^*]_{\mathcal{P}^+}\| \leq \|d(t)\| \end{aligned}$$

where we exploit (19), (26) and the fact that the projection is a non expansive map, that is

$$\|[x]_{\mathcal{P}^+} - [y]_{\mathcal{P}^+}\| \leq \|x - y\|;$$

- 2) if  $p_G(t+1) \in \mathcal{P}^+$ , then  $f(p_G(t+1)) \leq f(p_G(t))$  (it comes from Proposition 3.3 in [17]);
- 3) if  $p_G(t+1) \in \mathcal{P}^-$ , we cannot know if  $f(p_G(t+1)) \leq f(p_G(t))$ .  
Otherwise, if  $p_G(t) \in \mathcal{P}^-$  then
- 4) if  $p_G(t+1) \in \mathcal{P}^-$ , then  $\|d(t+1)\| \leq \|d(t)\|$  and  $f(p_G(t+1)) \leq f(p_G(t))$ . Let  $x \in \mathbb{R}^m$ , and let  $x_{\parallel}$  and  $x_{\perp}$  be the components of  $x$  parallel or orthogonal to  $\mathbf{1}$ , respectively.

Then it is trivial to see that  $\|d(t+1)\| \leq \|d(t)\|$  while  $\|d(t+1)_{\perp}\| = \|d(t)_{\perp}\|$ .

- 5) if  $p_G(t+1) \in \mathcal{P}^+$ , then we cannot know if  $\|d(t+1)\| \leq \|d(t)\|$  and  $f(p_G(t+1)) \leq f(p_G(t))$ . We point out that this is the only situation in which  $d$  could increase;

From the above considerations, we get that if the trajectory lies always in  $\mathcal{P}^+$ , (27) guarantees the convergence of the algorithm. Furthermore, if  $\exists T : \{p_G : \|p_G - p_G^*\| \leq d(T)\} \in \mathcal{P}^+$ , then from 1) and 2) it follows again the convergence of the algorithm. It is clear that, in principle, the only possible situation in which the algorithm does not converge, is the one in which there is a continuing sequence of cross of  $\mathcal{P}^0$ , from  $\mathcal{P}^-$  to  $\mathcal{P}^+$  because, we point it out again, it is the only situation in which  $d$  can increase. That is a motion with the following characteristics:

- (i) when  $p_G \in \mathcal{P}^+$ , then the trajectory of  $p_G$  approaches  $\mathcal{P}^0$ , always diminishing however the distance to  $p_G^*$  (due to 1) ), until  $p_G$  crosses it. The only condition that make it happens is that

$$\left\langle \frac{\partial \hat{f}}{\partial p_G}, \mathbf{1} \right\rangle \leq 0 \quad (29)$$

that is

$$\begin{aligned} \mathbf{1}^T \left( 2c_0 \frac{\cos(\theta)}{U_N^2} (M p_G + N p_L) + (c_G - c_0) \mathbf{1} \right) &= \\ &= (c_G - c_0) \mathbf{1}^T \mathbf{1} + o\left(\frac{1}{U_N}\right) = \\ &\simeq (c_G - c_0) m \leq 0 \end{aligned}$$

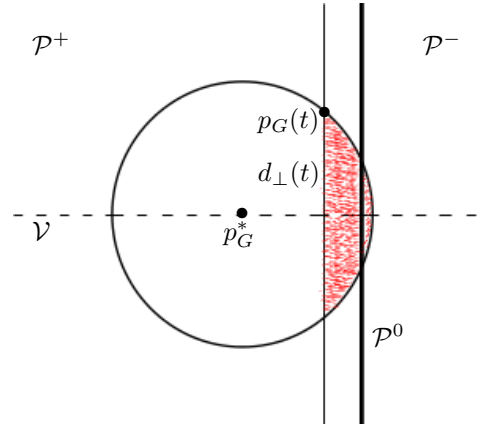


Fig. 5. Here we are in the case in which  $m = 2$ . Due to (28),  $p_G(t+1)$  will be inside the circle centered in  $p_G^*$  and passing through  $p_G(t)$ , while due to (29),  $p_G(t+1)$  will be on the right side of the vertical line passing through  $p_G(t)$ . As a consequence,  $p_G(t+1)$  will lie in the red dotted region, and then  $\|d_{\perp}(t+1)\| \leq \|d_{\perp}(t)\|$ . The dashed line represents the variety  $\mathcal{V}$ .

and then this type of trajectory is possible only when  $c_0 > c_G$ . If otherwise  $c_G > c_0$ , then the update of  $p_G$  does not point  $\mathcal{P}^-$  and then the trajectory will evolve only in  $\mathcal{P}^+$  and (27) guarantees the convergence of the algorithm.

- (ii) when  $p_G \in \mathcal{P}^-$ , then the trajectory of  $p_G$  approaches  $\mathcal{P}^0$ , always diminishing however the distance to  $p_G^*$  (due to 4) ), until  $p_G$  crosses it, producing an increasing in the distance among  $p_G$  and  $p_G^*$ ;
- (iii) points (i) and (ii) repeat continuously, and it is just the transition from  $\mathcal{P}^-$  to  $\mathcal{P}^+$  that makes the distance increase and the algorithm not to converge

Now we will show that, if (27) holds the former motion cannot last always. First of all, exploiting (14) and being all  $p_G \in \mathcal{P}^0$  such that

$$\begin{aligned} 0 &= -\mathbf{1}^T p_G - \mathbf{1}^T p_L + \ell(s_G, s_L, U_N) \\ &= -\mathbf{1}^T p_G - \mathbf{1}^T p_L + o\left(\frac{1}{U_N}\right) \end{aligned}$$

we approximate  $\mathcal{P}^0$  with the set of all  $p_G$  such that  $\mathbf{1}^T p_G + \mathbf{1}^T p_L = 0$ . Suppose now that a trajectory like the one described above takes place. Consider the evolution of  $d_{\perp}(t)$ . We have that  $d_{\perp}(t) = (I - \mathbf{1}\mathbf{1}^T/m)d(t) = P_{\perp}d(t)$ , where  $P_{\perp}$  is the projection matrix onto the space orthogonal to  $\mathbf{1}$ . If we define the variety

$$\mathcal{V} = \{p_G : p_G = p_G^* + v, v \in (\ker \mathbf{1})^{\perp}\}$$

then  $d_{\perp}$  represents the distance among  $p_G$  and  $\mathcal{V}$ .

- 1) if  $p_G \in \mathcal{P}^+$ , then (28) and (29) force  $d_{\perp}$  to decrease. The condition is well depicted in Figure 1.
- 2) if  $p_G \in \mathcal{P}^-$ , then until  $p_G$  remain in  $\mathcal{P}^-$  then  $d_{\perp}$  maintains its value, because

$$P_{\perp} \frac{\partial \hat{f}}{\partial p_G} = c_G P_{\perp} \mathbf{1} = 0$$

i.e. the motion takes place in a subspace orthogonal to  $\mathbf{1}$ .

From the previous consideration, it turns out that the trajectory tends to the variety  $\mathcal{V}$  that intersects  $\mathcal{P}^0$  in  $[p_G^*]_{\mathcal{P}^0}$ , where  $[\cdot]_{\mathcal{P}^0}$  is the projection into  $\mathcal{P}^0$ . Notice that the set

$$\Phi = \{p_G : \|p_G - p_G^*\| \leq \|[p_G^*]_{\mathcal{P}^0} - p_G^*\|\}$$

that represents the ball centered in  $p_G^*$  and with radius  $\|[p_G^*]_{\mathcal{P}^0} - p_G^*\|$  lies inside  $\mathcal{P}^+$  and it is tangent to  $\mathcal{P}^0$  in  $[p_G^*]_{\mathcal{P}^0}$ . The decreasing of  $d_\perp$  and the crosses from  $\mathcal{P}^-$  to  $\mathcal{P}^+$  force the trajectory to enter  $\Phi$ , and then (28) makes  $p_G$  to converge to  $p_G^*$ . ■

*Proof:* [Proof of Proposition 7]

The solution  $p_G^*$  of (15) belongs to  $\mathcal{P}^0$ , that is the discontinuity variety of  $\frac{\partial \hat{f}}{\partial p_G}$ , and the minimum of  $\hat{f}^+$  belongs to  $\mathcal{P}^-$ . This implies that, both in  $\mathcal{P}^+$  and  $\mathcal{P}^-$ , the opposite of  $\hat{f}$  gradient points  $\mathcal{P}^0$ . Then, if  $p_G(t) \in \mathcal{P}^+$  and we perform the projected gradient descent of  $\hat{f}^+$  ( $\hat{f}(p_G)$  is equal to  $\hat{f}^+(p_G)$  in  $\mathcal{P}^+$ ), in a finite time the trajectory hthe boundary  $\mathcal{P}^0$ . If, otherwise,  $p_G(t) \in \mathcal{P}^-$  again the projected gradient descent of  $\hat{f}^-$  ( $\hat{f}(p_G)$  is equal to  $\hat{f}^-(p_G)$  in  $\mathcal{P}^-$ ), will make  $p_G$  to cross  $\mathcal{P}^0$ . It is clear as a result that it borns a motion in which there is a continous cross of  $\mathcal{P}^0$ . Consider now the update equation

$$p_G(t+1) = p_G(t) - \gamma \frac{\partial \hat{f}}{\partial p_G}(p_G(t)) \quad (30)$$

that is simply (25) without the projection. It can be interpreted as the forward-Euler discrete-time version of the continous time update

$$\epsilon \dot{p}_G(t) = -\gamma \frac{\partial \hat{f}}{\partial p_G}(p_G(t)) \quad (31)$$

where  $\epsilon$  is the discretization time interval. If we apply the change of timescale

$$\tau = \frac{t}{\epsilon} \Rightarrow \frac{d\tau}{d\epsilon} = \frac{1}{\epsilon}$$

we obtain

$$\dot{p}_G(\tau) = -\gamma \frac{\partial \hat{f}}{\partial p_G}(p_G(\tau)) = \gamma \varphi(p_G(\tau)) \quad (32)$$

where

$$\varphi(p_G) = \begin{cases} \varphi^+ = c_0 \left( 2 \frac{\cos(\theta)}{U_N^2} (Mp_G + Np_L) \right) + \\ \quad + (c_G - c_0) \mathbf{1} & \text{if } p_G \in \mathcal{P}^+ \\ \varphi^- = c_G \mathbf{1} & \text{if } p_G \in \mathcal{P}^- \end{cases}$$

Equation (32) represents the continous time gradient descent of  $\hat{f}$ . If we fix a initial  $p_G$ , from the previous considerations in a finite time we reach  $\mathcal{P}^0$  and then, due to the nature of  $\hat{f}$  gradient, we have a sliding mode on the variety. Now we have to obtain a equivalent velocity. Again, as we did in the previous proof, we approximate  $\mathcal{P}^0$  with the set of all  $p_G$  such that  $\mathbf{1}^T p_G + \mathbf{1}^T p_L = 0$ . Now, following Filippov's continuation method [18], we have to find, among the convex combination of  $\varphi^+$  and  $\varphi^-$  "near"  $\mathcal{P}^0$  the one that maintains the trajectory in the variety, that is we have to find a  $\varphi^0$  such that

$$\varphi^0 = \mu \varphi^+ + (1 - \mu) \varphi^-, \quad \mathbf{1}^T \varphi^0 = 0$$

The former leads to the condition

$$\mu = \frac{c_G}{c_0} + o\left(\frac{1}{U_N}\right) \simeq \frac{c_G}{c_0}$$

from which it turns out that

$$\varphi^0 = 2c_G \frac{\cos(\theta)}{U_N^2} (Mp_G + Np_L)$$

and then, for all  $p_G(\tau)$  belonging to  $\mathcal{P}^0$ , the equivalent velocity is described

$$\dot{p}_G(\tau) = -\gamma 2c_G \frac{\cos(\theta)}{U_N^2} (Mp_G(\tau) + Np_L) \quad (33)$$

describes the sliding mode on  $\mathcal{P}^0$ . Notice that, from Lemma 5, we have that  $c_0 > c_G$  and then  $0 < \mu < 1$ . Now consider the discretized version of (33) constrained to the feasible set  $\mathcal{B}$

$$p_G(t+1) = \left[ p_G(\tau) - \epsilon \gamma 2c_G \frac{\cos(\theta)}{U_N^2} (Mp_G(t) + Np_L) \right]_{\mathcal{P}^0 \cap \mathcal{B}} \quad (34)$$

with  $\epsilon$  arbitrary small, and where  $[\cdot]_{\mathcal{P}^0 \cap \mathcal{B}}$  is the projection into  $\mathcal{P}^0 \cap \mathcal{B}$ . Let's define  $d(t) = [p_G(t)]_{\mathcal{P}^0} - p^*$ , i.e.  $d(t)$  represents the distance among the agents state  $p_G(t)$  and the solution of (15). The equilibrium  $p_G^*$  satisfies

$$\tilde{p}_G^* = \left[ \tilde{p}_G^* - \epsilon \gamma 2c_G \frac{\cos(\theta)}{U_N^2} (M\tilde{p}_G^* + Np_L) \right]_{\mathcal{P}^0 \cap \mathcal{B}} \quad (35)$$

We have that

$$\|d(t+1)\| \leq \left\| \left( I - \epsilon \gamma 2c_G \frac{\cos(\theta)}{U_N^2} M \right) \right\| \|d(t)\|$$

being the projection a non expansive map ( $\|[x]_{\mathcal{P}^0} - [y]_{\mathcal{P}^0}\| \leq \|x - y\|$ ). Thus, being  $\epsilon$  arbitrary small and  $M$  a symmetric positive definite matrix, we have  $\|d(t+1)\| < \|d(t)\|$  and then  $p_G(t)$  converges to  $p_G^*$ . ■

## REFERENCES

- [1] A. Ipakchi and F. Albuyeh, "Grid of the future," *Power and Energy Magazine, IEEE*, vol. 7, no. 2, pp. 52–62, 2009.
- [2] S. Grijalva and M. U. Tariq, "Prosumer-based smart grid architecture enables a flat, sustainable electricity industry," in *Innovative Smart Grid Technologies (ISGT), 2011 IEEE PES*. IEEE, 2011, pp. 1–6.
- [3] F. Katiraei and M. Irvani, "Power management strategies for a microgrid with multiple distributed generation units," *Power Systems, IEEE Transactions on*, vol. 21, no. 4, pp. 1821–1831, 2006.
- [4] P. Šulc, S. Backhaus, and M. Chertkov, "Optimal distributed control of reactive power via the alternating direction method of multipliers," *arXiv preprint arXiv:1310.5748*, 2013.
- [5] A. Lam, B. Zhang, and D. N. Tse, "Distributed algorithms for optimal power flow problem," in *Decision and Control (CDC), 2012 IEEE 51st Annual Conference on*. IEEE, 2012, pp. 430–437.
- [6] E. Dall'Anese, H. Zhu, and G. B. Giannakis, "Distributed optimal power flow for smart microgrids," 2013.
- [7] S. Bolognani, R. Carli, G. Cavraro, and S. Zampieri, "A distributed control strategy for optimal reactive power flow with power constraints," in *Conference on Decision and Control (CDC13), Conference on Decision and Control (CDC12)*, 2013.
- [8] —, "A distributed control strategy for optimal reactive power flow with power and voltage constraints," in *Smart Grid Communications (SmartGridComm), 2013 IEEE International Conference on*. IEEE, 2013, pp. 115–120.
- [9] A. G. Phadke, "Synchronized phasor measurements—a historical overview," in *Transmission and Distribution Conference and Exhibition 2002: Asia Pacific. IEEE/PES*, vol. 1. IEEE, 2002, pp. 476–479.

- [10] S. Bolognani and S. Zampieri, "A distributed control strategy for reactive power compensation in smart microgrids," *IEEE Trans. on Automatic Control*, vol. 58, no. 11, November 2013.
- [11] E. Devane and I. Lestas, "Stability and convergence of distributed algorithms for the opf problem," in *52nd IEEE Conference on Decision and Control*, 2013.
- [12] J. Lavaei and S. Low, "Zero duality gap in optimal power flow problem," *IEEE Transactions on Power Systems*, 2012.
- [13] E. Mallada and A. Tang, "Dynamics-aware optimal power flow," in *52nd IEEE Conference on Decision and Control*, 2013.
- [14] G. Cavraro and L. Badia, "A game theory framework for active power injection management with voltage boundary in smart grids," in *European Control Conference ECC 2013*, 2013.
- [15] W. H. Kersting, "Radial distribution test feeders," in *Power Engineering Society Winter Meeting, 2001. IEEE*, vol. 2. IEEE, 2001, pp. 908–912.
- [16] R. D. Zimmerman, C. E. Murillo-Sánchez, and R. J. Thomas, "MATPOWER: steady-state operations, planning and analysis tools for power systems research and education," *IEEE Transactions on Power Systems*, vol. 26, no. 1, pp. 12–19, Feb. 2011.
- [17] D. P. Bertsekas and J. N. Tsitsiklis, *Parallel and Distributed Computation: Numerical Methods*. Athena Scientific, 1997.
- [18] V. I. Utkin, *Sliding modes and their application in variable structure systems*. Mir Publishers, 1978.